PRAMANA
— journal of
physics

© Indian Academy of Sciences

Vol. 54, No. 6
June 2000
pp. 827–844

Effect of polarization on population transfer in H_2 by stimulated Raman transition with partially overlapping laser pulses

SWARALIPI GHOSH, SANJAY SEN, S S BHATTACHARYYA and SAMIR SAHA
Atomic and Molecular Physics Section, Department of Materials Science, Indian Association for the Cultivation of Science, Jadavpur, Calcutta 700 032, India

MS received 14 March 2000; revised 3 June 2000

Abstract. Polarization effects on population transfer by stimulated Raman transition using overlapping time dependent pump and Stokes laser pulses from the ground $X^1\Sigma_g^+(\nu_g = 0, J_g = 1)$ level of H_2 to the final $X^1\Sigma_g^+(\nu_f = 1, J_f = 1)$ level via the intermediate $B^1\Sigma_u^+(\nu_i = 14, J_i = 0, 2)$, $C^1\Pi_u^+(\nu_i = 3, J_i = 2)$ and $C^1\Pi_u^-(\nu_i = 3, J_i = 1)$ levels have been theoretically investigated by applying the density matrix formalism. We have studied in detail the dependence of the population transfer on time delay between two pulses for the cases of on-resonance excitations considering linear parallel and same-sense circular polarizations of the fields. The pump and Stokes fields are taken as having Gaussian pulse shapes with peak intensities $I_P^0(I_S^0) = 2 \times 10^6$ and 1×10^7 W/cm^2. Density matrix equations have been solved for each value of the magnetic quantum number $M_g(0, \pm 1)$ of the initial ground level taking into account the M_g dependence of the Rabi frequencies. M_g – averaged population transfer to the final level has also been calculated. For resonance excitations to the $B(14, 0)$ or $C(3, 1)$ levels, appreciable population transfer is achieved for intuitive pulse order for some particular values of M_g and M_i (magnetic quantum number of the resonant intermediate level) depending on the nature of polarizations. The calculated values of M_g – averaged population transfer for the two cases of polarizations show that for on-resonance excitation to the $B(14, 0)$ or the $C(3, 1)$ level, linear parallel polarization of the laser fields yield more transfer efficiency whereas for resonance excitation to the $B(14, 2)$ level, larger population transfer results from the same-sense circular polarizations. For resonance excitation to the $C(3, 2)$ level, M_g – averaged population is found to be almost polarization independent. The calculations for the six-level H_2 system reveal some interesting features of polarization effects on the population transfer efficiency.

Keywords. Population transfer; polarization effects; stimulated Raman transition.

PACS Nos 42.50.Hz; 33.80.Be; 42.65.Dr

1. Introduction

The current interest in molecular dynamics, particularly with regard to reactive and nonreactive scattering, has produced the demand for a technique to produce atoms and molecules in specified quantum states. Techniques based upon adiabatic passage, via controlled temporal variation of the matrix elements of the Hamiltonian, offer possibilities for producing

complete population transfer to excited states. A valuable example of adiabatic population manipulation, termed stimulated Raman adiabatic passage (STIRAP), has been extensively discussed theoretically [1–9] and demonstrated experimentally [10]. In its elementary form, the STIRAP process takes place in a nondegenerate three-state system, coupled to two pulsed radiation fields (termed pump and Stokes fields) in a conventional Raman configuration (sometimes termed a Λ system). Through adiabatic evolution of the field dressed eigenstates, which go to two different levels at the beginning and end of the pulses, one can force complete population transfer between initial and final levels for counterintuitive sequence of pulses when the pump frequency is either on-resonance or off-resonance with the intermediate excited level. At no time during the transfer process appreciable population resides in the intermediate level. STIRAP has been successfully used for efficient and selective vibrational population transfer in sodium dimers [10(b)] and for transfer to excited electronic states in neon atoms [10(c)], both species providing fairly ideal three-level system.

Some very new and interesting phenomena were noticed when some of the states involved have nonzero angular momentum. Bergmann and coworkers studied numerically [11] a different as well as important multilevel aspect of the STIRAP procedure, involving the magnetic sublevel structure that accompanies rotational degeneracy and in a subsequent work they presented an algebraic analysis [12] of some of the features that are of particular importance for successful population transfer. They have also experimentally verified [13] their theoretical results.

In a previous paper [14], we have studied the nonadiabatic (NA) interaction effects on the population transfer in a four-level H_2 system by stimulated Raman transition from the ground $X^1\Sigma_g^+(\nu_g = 0, J_g = 0)$ level to the final $X^1\Sigma_g^+(\nu_f = 1, 2, J_f = 0, 2)$ levels via the intermediate $B^1\Sigma_u^+(\nu_i = 14, J_i = 1)$ and $C^1\Pi_u^+(\nu_i = 3, J_i = 1)$ levels coupled strongly by NA interaction. Both the fields were taken to be linearly polarized in the same direction. We have observed some interesting features due to the effects of the NA interaction.

In the present work, our objective is to investigate the influence of different polarizations of the pump and Stokes fields on the population transfer in a six-level H_2 system. To our knowledge, this is the first work where such calculations are done for a real six-level molecular system with four closely spaced intermediate levels belonging to the Σ^+ and $\Pi^\pm$ states. The H_2 molecule is chosen since its electronic potential energies and transition dipole moments are well-known so that an almost exact and detailed calculation on various aspects of population transfer can be performed. The density matrix formalism has been adopted for this study. It is a unique method for treating dynamics of multilevel systems interacting with external time-dependent fields in the presence of relaxations [1]. All decay rates of the intermediate levels due to spontaneous radiative emission to the initial and final levels alongwith the relaxations out of the six-level system have been incorporated explicitly.

Specifically, the calculations of population transfer have been performed from the ground $X^1\Sigma_g^+(\nu_g = 0, J_g = 1)$ level to the final $X^1\Sigma_g^+(\nu_f = 1, J_f = 1)$ level via the intermediate $B^1\Sigma_u^+(\nu_i = 14, J_i = 0, 2)$, $C^1\Pi_u^+(\nu_i = 3, J_i = 2)$ and $C^1\Pi_u^-(\nu_i = 3, J_i = 1)$ levels of H_2 for linear parallel and circular (same sense) polarizations of the pump and Stokes lasers. We have included the magnetic quantum number dependence of all the Rabi frequencies. We have studied the dependence of the population transfer on time delay between the pump and Stokes fields for the case of on-resonance at peak intensities

$I_P^0(I_S^0) = 2 \times 10^6$ and 1×10^7 W/cm^2 of the pump (Stokes) fields. The fields are assumed to have the same peak intensity, pulse shape and duration.

We have performed the entire density matrix calculations for each value of $M_g(0, \pm 1)$ of the ground level. To obtain the M-independent population transfer, we have summed the final level populations over M_f and averaged them over M_g. It may be mentioned here that in our investigation, we have also incorporated the nonadiabatic coupling between the two intermediate $B(14, 2)$ and $C(3, 2)$ levels due to intermolecular configuration interaction [14]. The present work reveals some interesting features of the effect of different polarizations of the laser fields on the population transfer efficiency.

2. Formulation

This section discusses the formulation of the density matrix equations for the calculation of population transfer in H_2 by stimulated Raman transition from the ground $X\,^1\Sigma_g^+(\nu_g = 0, J_g = 1)$ level to higher vibrational level $(\nu_f = 1, J_f = 1)$ of $X^1\Sigma_g^+$ electronic state via excited intermediate levels $B^1\Sigma_u^+(\nu_i = 14, J_i = 0, 2)$, $C^1\Pi_u^+(\nu_i = 3, J_i = 2)$ and $C^1\Pi_u^-(\nu_i = 3, J_i = 1)$ under the action of time-dependent overlapping pump and Stokes laser pulses. The scheme considered here for population transfer process is schematically shown in figure 1 where all the state-labels, the relevant Rabi frequencies as well as spontaneous decay rates are specified. Here the ground and final (terminal) levels are designated as $|0\rangle$ and $|5\rangle$, respectively. Two intermediate levels ($\nu_i = 14$; $J_i = 0$ and 2) belonging to the $B^1\Sigma_u^+$ electronic state are denoted by $|1\rangle$ and $|2\rangle$, respectively, while $|3\rangle$ and $|4\rangle$ specify the respective levels $C^1\Pi_u^+(\nu_i = 3, J_i = 2)$ and $C^1\Pi_u^-(\nu_i = 3, J_i = 1)$. Among these four intermediate levels, the two new perturbed eigenlevels $B\,^1\Sigma_u^+(\nu_i = 14, J_i = 2)$ and $C^1\Pi_u^+(\nu_i = 3, J_i = 2)$ are generated due to the mixing of the two closely spaced adiabatic Born–Oppenheimer (ABO) levels $\nu = 14$, $J = 2$ of B state and $\nu = 3$, $J = 2$ of C state, through the nonadiabatic (NA) electronic-rotational interaction. The perturbed $B(14, 2)$ level has $\sim 87\%$ B character and $\sim 13\%$ C character whereas the perturbed $C(3, 2)$ level has $\sim 87\%$ C character and $\sim 13\%$ B character [15] implying a rather weak NA mixing. Level $|0\rangle$ is coupled with the four intermediate levels through the absorption of a photon of the pump field whereas the Stokes field drives the transition from the intermediate levels to final level $|5\rangle$. $|0\rangle$ and $|5\rangle$ being the levels of same parity, the transition between them is electric dipole forbidden.

The Liouville equation for the density matrix operator $(\rho(t))$ of the six-level system interacting with two time-dependent realistic laser pulses including phenomenologically decay rates (Γ) due to spontaneous emission, is given by (in a.u.)

$$\frac{\mathrm{d}\rho(t)}{\mathrm{d}t} = -i[H, \rho] - \Gamma\rho, \tag{1}$$

where $H(t) = H_0 + H_I(t) + H_{\mathrm{NA}}$ is the total time-dependent Hamiltonian of the system. H_0 is the Hamiltonian of the unperturbed molecule and $H_I(t)$ denotes the interaction Hamiltonian between the molecule and the fields, which in the electric field or length gauge form (with dipole approximation) can be expressed as

$$H_I(t) = -\vec{E}_P(t) \cdot \vec{d} - \vec{E}_S(t) \cdot \vec{d}. \tag{2}$$

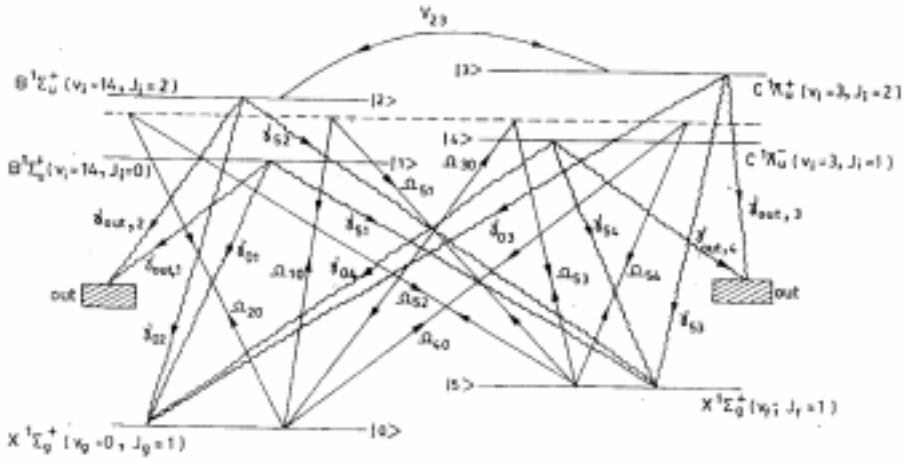

Figure 1. Schematic diagram of the six-level H_2 system interacting with the pump and Stokes lasers where all state labels, the relevant Rabi frequencies as well as the spontaneous decay rates are indicated. Ω_{ji} denotes the time-dependent one-photon coupling matrix element for Rabi transition from level $|i\rangle$ to level $|j\rangle$ by the pump or Stokes field. V_{23} is the nonadiabatic interaction matrix element between $|2\rangle$ and $|3\rangle$. γ_{0n} and γ_{5n} $(n = 1\text{–}4)$ denote the spontaneous radiative decay rates from level $|n\rangle$ to levels $|0\rangle$ and $|5\rangle$. $\gamma_{\mathrm{out},n}$ denotes the decay rates of level $|n\rangle$ to other levels out of the six-level system considered.

$\vec{d}$ denotes the transition dipole operator whereas $\vec{E}_P(t)$ and $\vec{E}_S(t)$ are the time-dependent electric field vectors of the pump and Stokes lasers, respectively. Considering the parallel–parallel ($\updownarrow\updownarrow$) and same sense circular ($\circlearrowright\circlearrowright$) polarizations of the pump and Stokes beams, the classical forms of $\vec{E}_P(t)$ and $\vec{E}_S(t)$ are given by

$$\vec{E}_P(t) = \frac{1}{2} f_P(t) F_P^0 [\hat{\varepsilon}_P \mathrm{e}^{i\omega_P t} + \hat{\varepsilon}_P^* \mathrm{e}^{-i\omega_P t}] \tag{3a}$$

and

$$\vec{E}_S(t) = \frac{1}{2} f_S(t) F_S^0 [\hat{\varepsilon}_S \mathrm{e}^{i\omega_S t} + \hat{\varepsilon}_S^* \mathrm{e}^{-i\omega_S t}], \tag{3b}$$

where ω_P and ω_S are, respectively, the pump and Stokes frequencies and $\hat{\varepsilon}_P$ and $\hat{\varepsilon}_S$ are the corresponding unit polarization vectors. $f_P(t)$ and $f_S(t)$ express the time variation of the field amplitudes of peak values F_P^0 and F_S^0, respectively. The functional forms of $f_P(t)$ and $f_S(t)$ are taken to be Gaussian [1] with full width (FWHM) τ_p,

$$f_P(t) = \exp[-(t - t_p)^2 / 2\tau_p^2] \tag{4a}$$

and

$$f_S(t) = \exp[-\{t - (t_p + \Delta t)\}^2 / 2\tau_p^2]. \tag{4b}$$

Δt introduces the time delay between the pulses. $\Delta t > 0$ specifies the intuitive pulse order in which the pump pulse preceeds the Stokes pulse whereas $\Delta t < 0$ corresponds to the counterintuitive sequence of interaction which begins with the Stokes pulse and ends with the pump pulse. t_p is the pulse scaling time.

With these definitions in hand and starting from the Liouville equation (1), the optical Bloch equations for the elements of density matrix operator $\rho(t)$ describing the dynamics of the six-level system, within the rotating wave approximation (RWA), can be written as

$$\dot{\sigma}_{nn} = -\sum_{n'=1}^{4} [i(\Omega_{nn'}\sigma_{n'n} - \Omega_{n'n}\sigma_{nn'}) - \gamma_{nn'}\sigma_{n'n'}]; \quad n = 0, 5 \tag{5a}$$

$$\dot{\sigma}_{n0} = -i \sum_{n'=0,5} \Omega_{nn'}\sigma_{n'0} + i \sum_{n'=1}^{4} \Omega_{n'0}\sigma_{nn'} + \left(i\Delta_n - \frac{1}{2}\Gamma_n\right)\sigma_{n0}$$
$$-i(V_{n,n+1}\sigma_{n+1,0}\delta_{n2} + V_{n,n-1}\sigma_{n-1,0}\delta_{n3}); \quad n = 1 - 4 \tag{5b}$$

$$\dot{\sigma}_{50} = -i \sum_{n'=1}^{4} (\Omega_{5n'}\sigma_{n'0} - \Omega_{n'0}\sigma_{5n'}) + i(\Delta)\sigma_{50}, \tag{5c}$$

$$\dot{\sigma}_{5n} = i \sum_{n'=0,5} \Omega_{n'n}\sigma_{5n'} - i \sum_{n'=1}^{4} \Omega_{5n'}\sigma_{n'n} + \left[i\{(\omega_n - \omega_5) - \omega_S\} - \frac{1}{2}\Gamma_n\right]\sigma_{5n}$$
$$+i(V_{n+1,n}\sigma_{5,n+1}\delta_{n2} + V_{n-1,n}\sigma_{5,n-1}\delta_{n3}); \quad n = 1 - 4 \tag{5d}$$

$$\dot{\sigma}_{nn'} = -i \sum_{n''=0,5} (\Omega_{nn''}\sigma_{n''n'} - \Omega_{n''n'}\sigma_{nn''}) + \left[i(\omega_{n'} - \omega_n) - \frac{1}{2}(\Gamma_{n'} + \Gamma_n)\right]\sigma_{nn'}$$
$$-i(V_{n,n+1}\sigma_{n+1,n'}\delta_{n2} + V_{n,n-1}, \sigma_{n-1,n'}\delta_{n3})$$
$$+i(V_{n'+1,n'}\sigma_{n,n'+1}\delta_{n'2} + V_{n'-1,n'}\sigma_{n,n'-1}\delta_{n'3}). \qquad n, n' = 1 - 4 \tag{5e}$$

The rest of the total 36 equations are obtained by using the relation $\sigma_{nn'} = \sigma^*_{n'n}$. $\sigma(t)$ is the slowly varying matrix operator whose elements are related to those of $\rho(t)$ by the defining equations $\rho_{nn}(t) = \sigma_{nn}(t)$, $\rho_{n0}(t) = \sigma_{n0}(t)\mathrm{e}^{-i\omega_p t}$, etc. $\Omega_{n'n}$ denotes the time-dependent one-photon coupling matrix element for transition from the state $|n\rangle$ to the state $|n'\rangle$ by the pump or Stokes field. $V_{23}(= -22.60\ \mathrm{cm}^{-1})$ is the time-independent nonadiabatic coupling matrix element between the two ABO levels $\nu = 14$, $J = 2$ of B state and $\nu = 3$, $J = 2$ of C state arising due to the configuration interaction between the two electronic states B and C [14]. $\Delta_n(n = 1\text{–}4)$ is the detuning of the pump laser frequency from the (unperturbed) energy difference between levels $|n\rangle$ and $|0\rangle$ and is expressed by $\Delta_n = \omega_P - (E_n - E_0)$. E_0 is the energy of the ground level $|0\rangle$ and E_n's are the (adiabatic) energies of levels $|n\rangle$. The expression for Δ is given by $\Delta = (\omega_P - \omega_S) - (E_5 - E_0)$ where E_5 is the energy of the final level $|5\rangle$. For two-photon Raman resonance, $\Delta = 0$. The diagonal elements $\sigma_{nn}(t)$ for $n = 0$ and 5, in eq. (5a), denote the populations of the

initial and final levels respectively, while the diagonal elements $\sigma_{nn'}(t)$ for $n' = n = 1$–4, in eq. (5e), give the populations of the corresponding four intermediate levels. The off-diagonal elements $\sigma_{n0}, \sigma_{5n}, \sigma_{nn'}(n' \neq n)$ for $n(n') = 1$–4 and σ_{50}, in eqs (5b)–(5e), are interpreted as the coherences. Γ_n $(n = 1$–$4)$ represent the total radiative decay rates of the levels $|n\rangle$. The term Γ_n introduces a coherence loss in the transfer process. Along with the spontaneous decay to the ground and final levels, each of the intermediate levels can decay to other levels out of this six-level system. The spontaneous emission from level $|n\rangle$ to levels $|0\rangle$ and $|5\rangle$ are explicitly represented by the decay rates γ_{0n} and γ_{5n}. The relaxations $(\gamma_{\mathrm{out},n})$ to other levels out of the six-level system are taken into account in the corresponding $\Gamma_n (= \gamma_{0n} + \gamma_{5n} + \gamma_{\mathrm{out},n})$. We have neglected photodissociation/photoionization of the molecules from the intermediate states. This is justified at the level of fluences that we have considered. The two-photon ionization out of the ground state will not contribute either. Since we are concerned here only with the on-resonance or near-resonance excitations and the intensities of the two pulsed fields are not too high, the ac Stark shifts of the intermediate levels as well as of the ground level have not been taken into consideration. We have also neglected the collisional relaxations of the intermediate and final levels since they are negligible in a beam experiment [10(a), (b)].

As Rabi frequency is a function of magnetic quantum number of the molecular levels involved in the transitions, we have carried out the entire six-level calculation for each M_g value separately and then have combined the results to get the averaged population of the final level.

The set of eqs (5) can be written in a matrix form as

$$\dot{\sigma} = M\sigma. \tag{6}$$

It may be noted that here M is a non-Hermitian and asymmetric matrix though $\Omega_{nn'} = \Omega^*_{nn'}$ and $V_{23} = V^*_{23}$.

Equation (6) can be solved in a similar way to that discussed in our earlier paper [14]. The evaluated diagonal elements $\sigma_{nn}(t),\ n = 0$–5 describe the populations at time t of the six-level system interacting with the two specified pulsed laser fields. Thus the final populations of the levels, viz. $P_g(J_g, M_g) = \sigma_{00}(\infty)$, $P_f(J_f, M_f) = \sigma_{55}(\infty)$ etc after the pulses are over can be evaluated.

The M_g – averaged population of the molecules in the final level is defined as

$$\bar{P}_f(J_f) = \frac{1}{2J_g + 1} \sum_{M_f = -J_f}^{J_f} P_f(J_f, M_f). \tag{7}$$

3. Calculations

We have calculated the population transfer in six-level H_2 system for Q-branch $(\Delta J = 0)$ fundamental $(\Delta\nu = 1)$ transition from the ground $X\,^1\Sigma_g^+(\nu_g = 0, J_g = 1)$ level to the final $X^1\Sigma_g^+(\nu_f = 1, J_f = 1)$ level via four excited intermediate levels $B\,^1\Sigma_u^+(\nu_i = 14, J_i = 0, 2)$, $C^1\Pi_u^+(\nu_i = 3, J_i = 2)$ and $C^1\Pi_u^-(\nu_i = 3, J_i = 1)$ considering the linear parallel (↕↕) and same sense circular (↻↻) polarizations of time-dependent overlapping pump and Stokes laser fields. The variation of transfer efficiency with the time displacement between

the two pulses are studied in detail assuming the peak intensities $[I^0_{P,S} = c(F^0_{P,S})^2/8\pi]$ of the pump (Stokes) fields as 2×10^6 W/cm^2 and 1×10^7 W/cm^2. The two laser pulses are assumed to have the same temporal shape and duration. The pulse width (FWHM) τ_p is taken as 170 ns so that the total spontaneous radiative relaxation from the intermediate levels can occur during the pulse duration. The calculated adiabatic (ABO) energies of the B and C intermediate levels are $E_1 = -12713.05$ cm^{-1}, $E_2 = -12643.03$ cm^{-1}, $E_3 = -12603.92$ cm^{-1}, $E_4 = -12706.88$ cm^{-1} respectively, with respect to the (ABO) threshold of the B/C state while the calculated ABO energies of the initial and final levels of the X state are $E_0 = -35999.85$ cm^{-1} and $E_5 = -31843.80$ cm^{-1} respectively, with respect to the (ABO) threshold of the X state. The wavelengths of the pump and Stokes lasers are about 94.7 and 98.6 nm, respectively. After performing the entire density matrix calculations for each $M_g(0, \pm 1)$ value of the ground level, M_g – averaged population of the molecules in the final level is calculated.

The Born–Oppenheimer (BO) potential energies and the adiabatic (AD) corrections to them for B, C, and X states are obtained from Wolniewicz and Dressler [16] and others [17]. Electronic transition dipole moments for $X - B(C)$ states are taken from Wolniewicz [18]. The potential and dipole moments are interpolated using the cubic spline interpolation method [19]. The radial bound wavefunctions are generated by solving numerically the radial Schrödinger equation with the well-known Numerov–Cooley method [20]. The Simpson integration rule is used to carry out the integrations for the single-photon matrix elements. Since we are interested in the detailed study of polarization effects on the population transfer process we had to consider both the radial and angular (polarization dependent) factors of different transition matrix elements. The nonadiabatic energies of $B(14, 2)$ and $C(3, 2)$ levels are given by Abgrall *et al* [15]. The values of the spontaneous decay rates $\gamma_{\mathrm{out},n}$ are obtained from Dalgarno and coworkers [21]. The radiative spontaneous emission from any discrete ro-vibrational level couples different possible rotational levels and their magnetic sublevels and each of them contributes differently in determining the values of the decay rates. We have incorporated J and M dependence properly in the values of γ_{0n}, γ_{5n} and Γ_n.

The magnitudes of the intensities used in the work (appearing in the Rabi frequencies Ω_{n0}, Ω_{5n}) are necessary to compensate/overcome the coherence losses (Γ_n) in the transfer process. The values of Ω_{n0}, Ω_{5n}, γ_{0n}, γ_{5n} and $\Gamma_n (n = 1\text{–}4)$ are given in tables 1 and 2 for $\updownarrow\updownarrow$ and $\circlearrowright\circlearrowright$ polarizations, respectively.

4. Results and discussions

In figures 2–5, the populations (P_f) in the final level for Q-branch $(\Delta J = 0)$ fundamental $(\Delta\nu = 1)$ transition from the initial $X^1\Sigma^+_g(\nu_g = 0, J_g = 1)$ to the final $X^1\Sigma^+_g(\nu_f = 1, J_f = 1)$ level via four excited intermediate levels (figure 1) in H_2 molecule are shown as a function of reduced time delay $(D = \Delta t/\tau_p)$ considering linear parallel $(\updownarrow\updownarrow)$ and circular (same sense $\circlearrowright\circlearrowright$) polarizations of the pump and Stokes laser fields. The profiles are investigated for two different values of peak intensities $I^0_P(I^0_S) = 2 \times 10^6$ and 1×10^7 W/cm^2 of pump (Stokes) pulses with FWHM width (τ_p) of the pulse as 170 ns and on-resonance excitations to the intermediate levels.

Figure 2a exhibits the population transfer for on-resonance excitation to the intermediate $B^1\Sigma^+_u(\nu_i = 14, J_i = 0)$ level and for $M_g = 0$ of the initial level. For the two

Table 1. Values (in cm^{-1}) of Rabi frequencies $(\Omega_{n'n})$, state-to-state spontaneous decay rates $(\gamma_{nn'})$ and total spontaneous decay rates $(\Gamma_{n'})$ for different transitions with linearly (parallel) polarized lasers. The intensities $I_P(I_S)$ are in W/cm^2.

	$M_g(M_f)=0$	$M_g(M_f)=\pm1$
Ω_{10}	$-6.07(-5)^*\sqrt{I_P}$	0
Ω_{20}	$-5.55(-5)\sqrt{I_P}$	$-4.81(-5)\sqrt{I_P}$
Ω_{30}	$1.08(-4)\sqrt{I_P}$	$9.37(-5)\sqrt{I_P}$
Ω_{40}	0	$-1.21(-4)\sqrt{I_P}$
Ω_{51}	$5.39(-5)\sqrt{I_S}$	0
Ω_{52}	$4.64(-5)\sqrt{I_S}$	$4.02(-5)\sqrt{I_S}$
Ω_{53}	$-2.07(-5)\sqrt{I_S}$	$-1.79(-5)\sqrt{I_S}$
Ω_{54}	0	$2.66(-5)\sqrt{I_S}$
γ_{01}	$1.28(-3)$	0
γ_{02}	$1.08(-3)$	8.08(−4)
γ_{03}	$4.09(-3)$	3.07(−3)
γ_{04}	0	5.08(−3)
γ_{51}	$8.98(-4)$	0
γ_{52}	$6.68(-4)$	5.01(−4)
γ_{53}	$1.32(-5)$	9.92(−5)
γ_{54}	0	2.18(−4)
Γ_1	$3.22(-2)$	3.00(−2)
Γ_2	$3.18(-2)$	3.13(−2)
Γ_3	$4.15(-2)$	4.05(−2)
Γ_4	$3.74(-2)$	4.27(−2)

$^* -6.07(-5) = -6.07 \times 10^{-5}$

Table 2. Values (in cm^{-1}) of Rabi frequencies $(\Omega_{n'n})$, state-to-state spontaneous decay rates $(\gamma_{nn'})$ and total spontaneous decay rates $(\Gamma_{n'})$ for different transitions with circularly (same-sense) polarized lasers. The intensities $I_P(I_S)$ are in W/cm^2.

	$M_g(M_f)=0$	$M_g(M_f)=+1$	$M_g(M_f)=-1$
Ω_{10}	0	0	$-6.07(-5)^*\sqrt{I_P}$
Ω_{20}	$4.81(-5)\sqrt{I_P}$	$6.80(-5)\sqrt{I_P}$	$2.78(-5)\sqrt{I_P}$
Ω_{30}	$-9.37(-5)\sqrt{I_P}$	$-1.32(-4)\sqrt{I_P}$	$-5.41(-5)\sqrt{I_P}$
Ω_{40}	$-1.21(-4)\sqrt{I_P}$	0	$-1.21(-4)\sqrt{I_P}$
Ω_{51}	0	0	$5.39(-5)\sqrt{I_S}$
Ω_{52}	$-4.02(-5)\sqrt{I_S}$	$-5.69(-5)\sqrt{I_S}$	$-2.32(-5)\sqrt{I_S}$
Ω_{53}	$1.79(-5)\sqrt{I_S}$	$2.53(-5)\sqrt{I_S}$	$1.03(-5)\sqrt{I_S}$
Ω_{54}	$2.66(-5)\sqrt{I_S}$	0	$2.66(-5)\sqrt{I_S}$
γ_{01}	0	0	$1.28(-3)$
γ_{02}	$8.08(-4)$	$1.61(-3)$	$2.69(-4)$
γ_{03}	$3.07(-3)$	$6.13(-3)$	$1.02(-3)$
γ_{04}	$5.08(-3)$	0	$5.08(-3)$
γ_{51}	0	0	$8.99(-4)$
γ_{52}	$5.01(-4)$	$1.00(-3)$	$1.67(-4)$
γ_{53}	$9.92(-5)$	$1.98(-4)$	$3.31(-5)$
γ_{54}	$2.18(-4)$	0	$2.18(-4)$
Γ_1	$3.00(-2)$	$3.00(-2)$	$3.22(-2)$
Γ_2	$3.13(-2)$	$3.26(-2)$	$3.04(-2)$
Γ_3	$4.05(-2)$	$4.37(-2)$	$3.84(-2)$
Γ_4	$4.27(-2)$	$3.74(-2)$	$4.27(-2)$

$^* -6.07(-5) = -6.07 \times 10^{-5}$

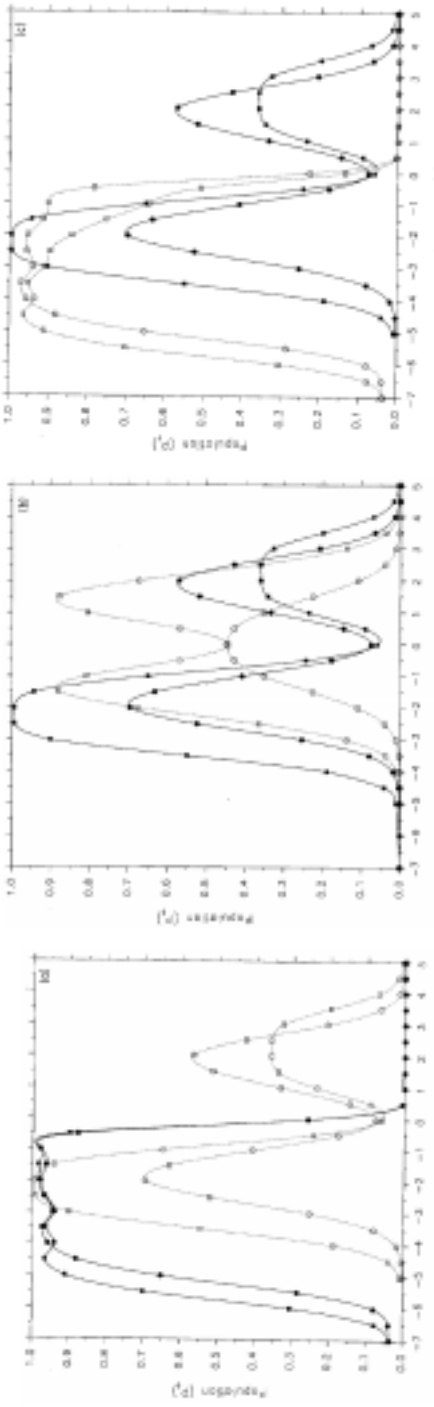

Figure 2. Population (P_f) of the final level plotted against (reduced) time delay ($D = \Delta t/\tau_p$) between the pulses for on-resonance excitation to the $B(14, 0)$ level for three different values of M_g with different peak intensities $I_P^0(I_S^0)$ and polarizations of the pulses. (**a**) $M_g = 0$, (**b**) $M_g = +1$, and (**c**) $M_g = -1$. Solid curves for linear parallel and dashed for circular polarizations. Circles for $I_P^0(I_S^0) = 2 \times 10^6$ W/cm^2, and squares for $I_P^0(I_S^0) = 1 \times 10^7$ W/cm^2.

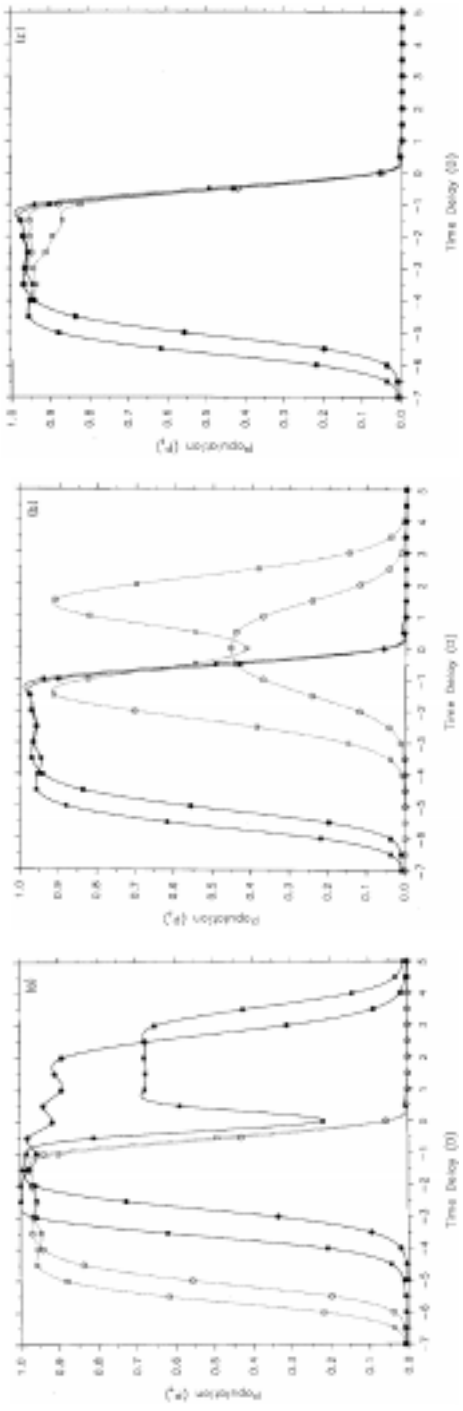

Figure 3. Same as figure 2 except for on-resonance excitation to the $C(3, 1)$ level.

different values of $I_P^0(I_S^0)$, the P_f profiles corresponding to the $\updownarrow\updownarrow$ polarizations have almost the same structure with a broad peak for the counterintuitive sequence of pulses and no transfer for intuitive pulse order. Nearly complete population transfer is achieved in the region $-4 \leq D \leq -1$ for both the intensities. The small oscillations in the peak region result from the presence of other intermediate levels which are energetically not far from the resonant level $B(14,0)$. For $\curvearrowright\curvearrowright$ polarizations, the profiles possess two peaks, one for the counterintuitive pulse order $(D < 0)$ and the other for the intuitive pulse order $(D > 0)$. The second peak for on-resonance excitation at intuitive pulse order is an interesting feature. It is worth mentioning here that this feature is not due to the effect of any nonadiabatic (NA) interaction as investigated in our earlier paper [14]. Though the resonance condition has been maintained here with $B(14,0)$ level, the Rabi frequency between $B(14,0)$ and the ground level vanishes for $M_g = 0$ and circular polarization with selection rule $\Delta M = M_i - M_g = +1$. But the matrix elements between the ground level and the other nearly intermediate levels $C(3,1)$, $B(14,2)$ and $C(3,2)$, which are now off-resonant do not vanish in this case. As a consequence, the population transfer curves show behaviour typical to the off-resonant excitation cases studied in our earlier work [14]. Thus, the different selection rules for linearly/circularly polarized radiations cause an important change in temporal dependence of the population transfer with polarization. For $\curvearrowright\curvearrowright$ polarizations, with the increase of $I_P^0(I_S^0)$, the maximum value of P_f is enhanced enormously around $D = -2$ for counterintuitive pulse order whereas for intuitive pulse order the peak height is decreased to a large extent at $D \approx +2$. About 68% transfer takes place for $I_P^0(I_S^0) = 2 \times 10^6$ W/cm^2 while for $I_P^0(I_S^0) = 1 \times 10^7$ W/cm^2 almost 100% transfer is obtained at $D \approx -2$.

Figure 2b presents the same data as figure 2a except for $M_g = +1$. Here P_f curves except the one for $\curvearrowright\curvearrowright$ polarizations with $I_P^0(I_S^0) = 2 \times 10^6$ W/cm^2, are found to have double peaks, one in the counterintuitive region and the other in the intuitive region. In this case the Rabi frequency Ω_{10} vanishes for both the polarizations considered and the system behaves like a off-resonantly excited one. For $\updownarrow\updownarrow$ polarizations, at $D \approx -2$ the transfer efficiency is about 0.68 at $I_P^0(I_S^0) = 2 \times 10^6$ W/cm^2 while it increases to nearly unity at $I_P^0(I_S^0) = 1 \times 10^7$ W/cm^2. The transfer efficiency at $D \approx +2$ is reduced from ~ 0.57 for $I_P^0(I_S^0) = 2 \times 10^6$ W/cm^2 to only ~ 0.36 when $I_P^0(I_S^0)$ is increased to 1×10^7 W/cm^2. For $\curvearrowright\curvearrowright$ polarization, the profiles are almost symmetrical for counterintuitive and intuitive pulse orders at both the intensities. The maximum transfer is only $\sim 44\%$ at $D = 0$ for $I_P^0(I_S^0) = 2 \times 10^6$ W/cm^2 while the population transfer is enhanced to $\sim 87\%$ at $D \approx \pm 1.5$ when $I_P^0(I_S^0)$ is increased to 1×10^7 W/cm^2. The relative magnitudes of the P_f profiles for different polarizations are mainly governed by the angular parts of the matrix elements for different relative transitions.

Figure 2c is same as figure 2a except for $M_g = -1$. Like the case for $M_g = 0$ and $\updownarrow\updownarrow$ polarizations (figure 2a), here the P_f profiles corresponding to $\curvearrowright\curvearrowright$ polarizations show a single broad peak in the counterintuitive region with almost total population transfer for both the intensities. This is because for $M_g = -1$ and $\curvearrowright\curvearrowright$ polarizations, the radiative transition matrix element Ω_{10} does exist as for $M_g = 0$ and $\updownarrow\updownarrow$ polarization and consequently, the P_f curves are similar to those obtained for the cases of on-resonance excitation in a three-level system [1] or our four-level system studied earlier [14], neglecting NA interaction.

It should be noticed here that the population profiles for $M_g = \pm 1$ and $\updownarrow\updownarrow$ polarizations (figure 2b–c) are identical to those for $M_g = 0$ and $\curvearrowright\curvearrowright$ polarizations (figure 2a) because

the polarization dependent angular factors of the different radiative transition matrix elements are same in both the cases. This can be verified by considering the M-dependent $3J$ coefficients appearing in the calculation of angular parts of the different matrix elements.

In figure 3a, we demonstrate the polarization dependence of the final level population for resonance excitation to the $C(3,1)$ level from $M_g = 0$ of the initial level. As the Rabi frequency corresponding to the radiative coupling between the initial and $C(3,1)$ level vanishes for $\updownarrow\updownarrow$ polarizations ($\Delta M = 0$), the respective curves show double peaked structure. For $I_P^0(I_S^0) = 2\times10^6$ W/cm^2, the two peaks merge so that about 97% transfer of population occurs at $D \approx -0.5$ and almost 95% transfer at $D \approx +0.5$. But for $I_P^0(I_S^0) = 1\times10^7$ W/cm^2, complete population is transferred to the final level around $D = -2$ for counterintuitive pulse order whereas only 69% transfer takes place around $D = +2$ for intuitive pulse order. For $\curvearrowright\curvearrowright$ polarizations, the Rabi frequency does not vanish and the population profiles have a single broad peak for $D < 0$ and are similar to the case of on-resonance excitation in three-level Na_2 system [1] or four level system studied earlier [14], assuming no NA interaction. This peak is rather insensitive to change in intensities.

Figure 3b is same as figure 3a except that the excitations are considered to take place from $M_g = +1$. For $\curvearrowright\curvearrowright$ polarizations, the profiles for both the intensities are symmetric about $D = 0$. For $I_P^0(I_S^0) = 2\times10^6$ W/cm^2 the maximum population transfer is only $\sim$ 44% at $D = 0$ while for $I_P^0(I_S^0) = 1\times10^7$ W/cm^2, it is $\sim$ 91% at $D = \mp1.5$. This behaviour of the curves can be understood in a way similar to that used in the discussion of the previous figures.

Figure 3c is same as figure 3a except for $M_g = -1$. Again, the curves are almost polarization independent with a broad peak in the counterintuitive region because the Rabi frequencies Ω_{40} between the ground and intermediate resonant $C(3,1)$ levels are the same for the two polarizations. In a narrow range near the peak region polarization seems to make a difference due to the presence of the other nearby intermediate levels. It may again be noticed here that the population transfer for $M_g = \pm1$ and $\updownarrow\updownarrow$ polarizations (figures 3b–c) is the same with that for $M_g = 0$ and $\curvearrowright\curvearrowright$ polarizations (figure 3a).

Figure 4a exhibits the P_f profiles against D corresponding to resonance with nonadiabatically perturbed $B(14,2)$ level for $M_g = 0$. Here the transfer efficiencies are significantly larger for $\updownarrow\updownarrow$ polarizations compared to those for $\curvearrowright\curvearrowright$ polarizations at all time delays. The higher value of the Rabi frequency Ω_{20} due to the higher angular factor for $\updownarrow\updownarrow$ polarizations leads to the present results. For $\updownarrow\updownarrow$ polarizations, the maximum transfer efficiencies are about 0.89 and 0.92, respectively for $I_P^0(I_S^0) = 2\times10^6$ W/cm^2 and 1×10^7 W/cm^2 with $D < 0$ while the corresponding efficiencies are about 0.41 and 0.73 for $\curvearrowright\curvearrowright$ polarizations.

Figure 4b is same as figure 4a except for $M_g = +1$. In this case the effects of polarizations on P_f profiles are reversed with respect to those in figure 4a. An interesting feature arises in the form of a small dip in the curve for $\curvearrowright\curvearrowright$ polarizations at $I_P^0(I_S^0) = 1\times10^7$ W/cm^2. This is due to the effect of the NA interaction (V_{23}) between the $B(14,2)$ and $C(3,2)$ levels. The effect is not very significant as the mixing due to the NA interaction is not so strong as in our earlier work [14].

Figure 4c is same as figure 4a except for $M_g = -1$. Almost complete population transfer occurs here around $D = -2$ for $\curvearrowright\curvearrowright$ polarizations irrespective of the values of the peak intensities whereas for $\updownarrow\updownarrow$ polarizations the maximum transfer efficiencies are about 0.42 and 0.71 for $I_P^0(I_S^0) = 2\times10^6$ W/cm^2 and 1×10^7 W/cm^2, respectively.

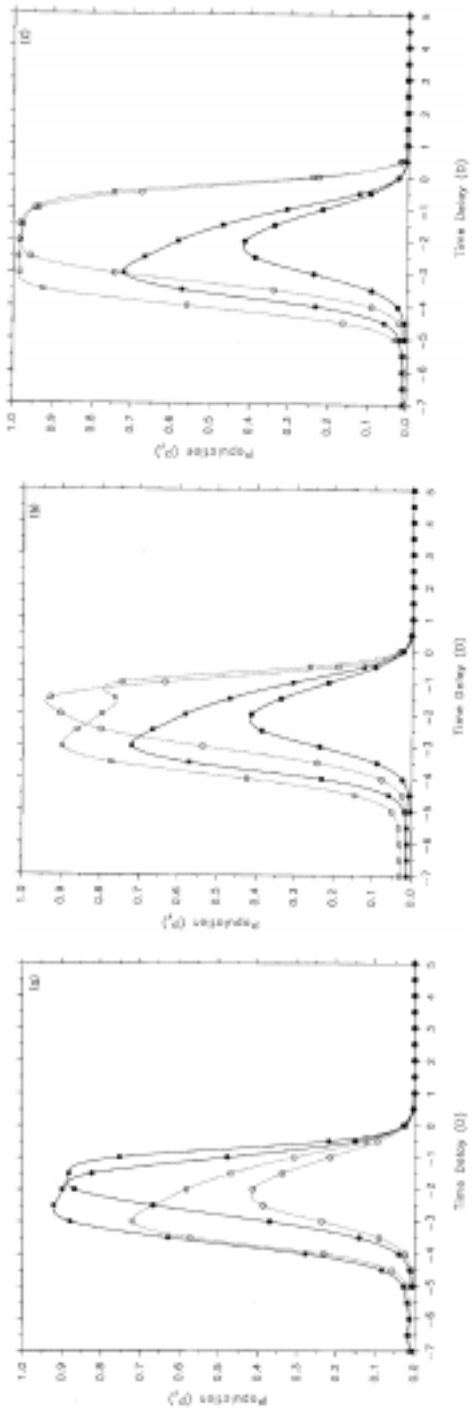

Figure 4. Same as figure 2 except for on-resonance excitation to the nonadiabatically perturbed $B(14, 2)$ level.

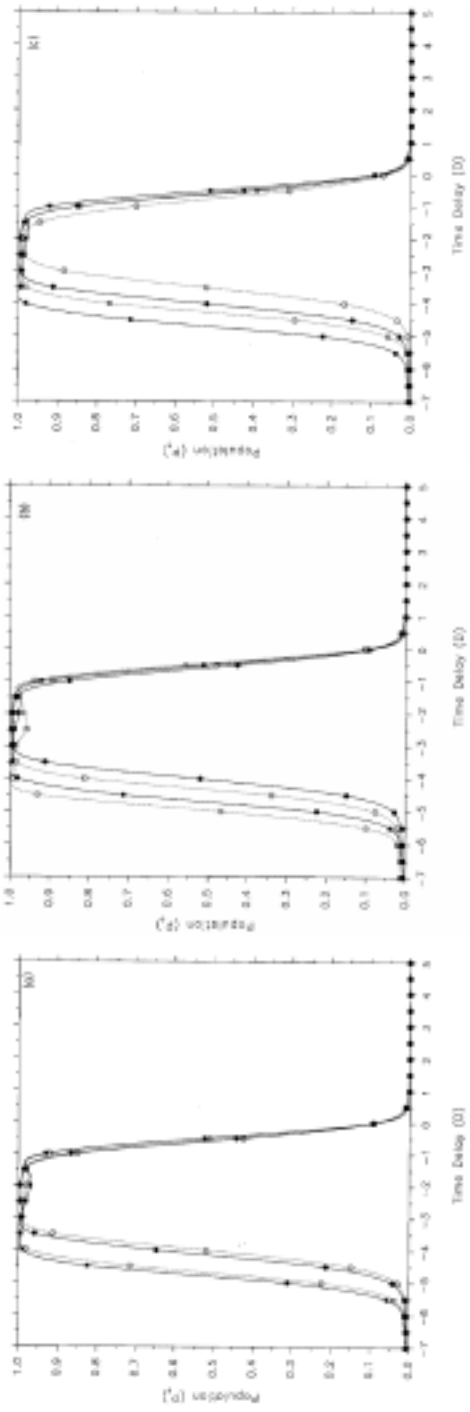

Figure 5. Same as figure 2 except for on-resonance excitation to the nonadiabatically perturbed $C(3,2)$ level.

Figures 5a–c present the P_f profiles for all three M_g considering the resonance excitation to the nonadiabatically perturbed $C(3,2)$ level. In each case of transition with different M_g, unit transfer efficiency is achieved for counterintuitive pulse sequence independent of the nature of polarizations of the fields and the values of $I_P^0(I_S^0)$. Since Ω_{20} or Ω_{30} does not vanish, the population profiles for on-resonance excitation to $C(3,2)$ or $B(14,2)$ level become similar to the case of on-resonance excitation in the three-level Na_2 system [1] or the four-level H_2 system investigated earlier [14], without any NA interaction.

Figures 6a–d show the M_g – averaged population $(\bar{P}_f)$ of the molecules in the final level for different on-resonance excitation cases discussed above, corresponding to resonance with $B(14,0)$, $C(3,1)$, the perturbed $B(14,2)$ and the perturbed $C(3,2)$ levels, respectively. It is seen that figures 6a and 6b exhibit double peaked distribution though the peaks for $D > 0$ are weak. The main peaks show a larger transfer for $\updownarrow\updownarrow$ polarizations. For resonance with the perturbed $B(14,2)$ level, the peak shows significant displacement with D as the intensity is changed. The transfer is much below the optimal at this pump frequency. In figure 6d, under the condition of an intermediate resonance with the perturbed $C(3,2)$ level, complete population transfers in a broad region around $D = -2.5$ take place for both intensities and polarizations. However, the curves for the higher intensities are broader and the rising portions of the curves shift to lower values of D as the intensities are increased.

About a decade ago, XUV lasers ($<$ 100 nm wavelength) of 50 ns pulse duration and 3×10^{12} W/cm^2 peak intensity were generated [22]. Earlier, VUV tunable ArF lasers of 55 ns pulse duration and 1.6×10^9 W/cm^2 peak intensity were generated with 193 nm wavelength [23]. We assume that experiments with the laser parameters similar to those used by us may be feasible.

5. Conclusions

We have presented a density matrix calculation showing how different polarizations of the pump and Stokes fields affect the population transfer in a six-level H_2 system for on-resonance excitations to various intermediate levels. For resonance excitation with the $B(14,0)$ or $C(3,1)$ level, the Rabi frequency (Ω_{10} or Ω_{40}) may vanish for some particular values of M_g and M_f (magnetic quantum numbers of the initial and resonant intermediate levels) depending on the nature of polarizations. In such situations, efficient population transfer for intuitive pulse order (i.e. $D > 0$) can be obtained. This is an interesting feature of population transfer arising from simple dipole selection rules. The calculated values of M_g – averaged population of the molecules in the final level for different combinations of polarizations show that for on-resonance excitation to the $B(14,0)$ or the $C(3,1)$ level, linear parallel polarizations of the laser fields yield more transfer efficiency whereas for the resonance excitation to the $B(14,2)$ level, larger population transfer results from the same-sense circular polarizations. For resonance excitation to the $C(3,2)$ level, the averaged population is found to be almost polarization independent. Thus, the polarizations of the laser fields do affect the outcome but differently at different frequencies of the lasers and we can control the population transfer by taking proper polarizations of the pump and Stokes fields.

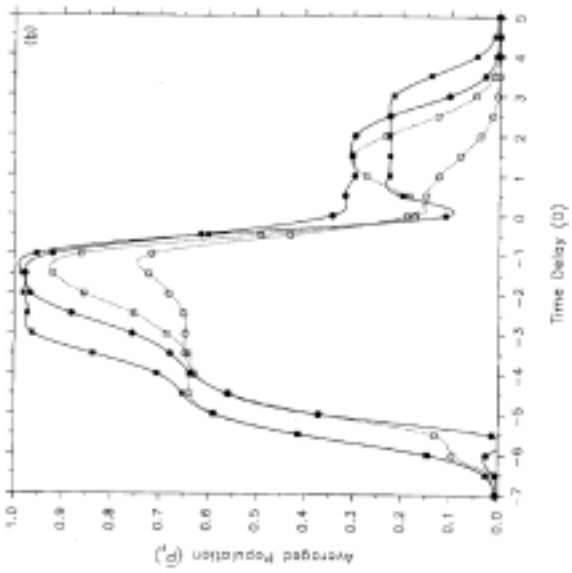

Figure 6b.

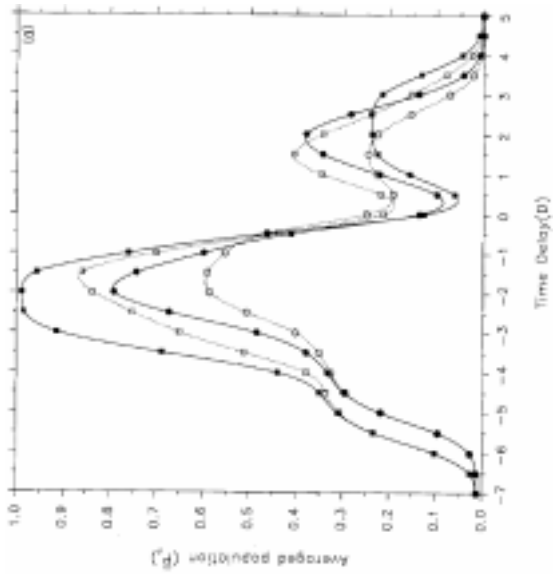

Figure 6a.

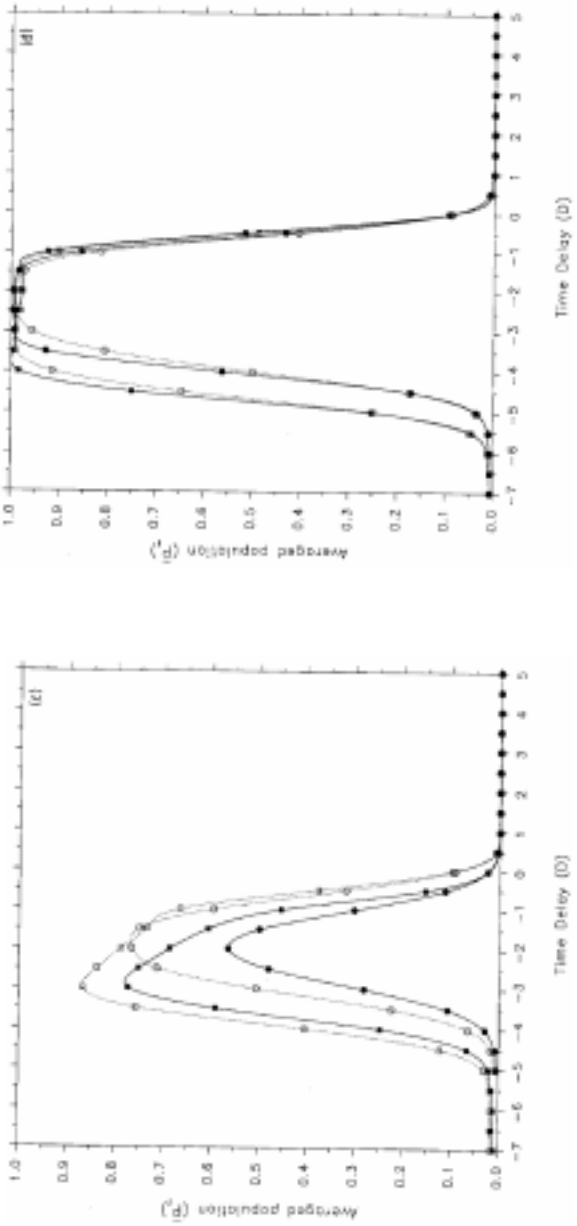

Figure 6. M_g – averaged population ($\bar{P}_f$) of the final level plotted against (reduced) time delay ($D = \Delta t/\tau_p$) between the pulses for on-resonance excitation to different intermediate levels with different peak intensities $I_P^0(I_S^0)$ and polarizations of the pulses. **(a)** $B(14,0)$, **(b)** $C(3,1)$, **(c)** nonadiabatically perturbed $B(14,2)$, and **(d)** nonadiabatically perturbed $C(3,2)$. Solid curves for linear parallel and dashed for circular polarizations. Circles for $I_P^0(I_S^0) = 2 \times 10^6$ W/cm^2, and squares for $I_P^0(I_S^0) = 1 \times 10^7$ W/cm^2.

We observe that in a multilevel system, there is appreciable population transfer with intuitive pulse order for linear/circular polarizations of the fields for on-resonance excitations to some of the intermediate levels. This is in contrast to the three-level system [1] or our four-level system (with $J_i = 0$) studied earlier [14], neglecting NA interaction. The physics behind it is the presence of neighbouring off-resonant intermediate levels and the vanishing of the transition matrix element of the on-resonant intermediate level due to different optical selection rules for linearly/circularly polarized light.

References

[1] Y B Band and P S Julienne, *J. Chem. Phys.* **94**, 5291 (1991); **95**, 5681 (1991); **97**, 9107 (1992)
Y B Band, *Phys. Rev.* **A45**, 6643 (1992)

[2] Y B Band and P S Julienne, *J. Chem. Phys.* **96**, 3339 (1992)

[3] N V Vitanov and S Stenholm, *Opt. Commun.* **127**, 215 (1996); **135**, 394 (1997); *Phys. Rev.* **A55**, 648 (1997); **55**, 2982 (1997); **56**, 741 (1997); **56**, 1463 (1997)

[4] R G Unanyan, N V Vitanov and S Stenholm, *Phys. Rev.* **A57**, 462 (1998)

[5] A Kuhn, G Coulston, G Z He, S Schiemann, K Bergmann and W S Warren, *J. Chem. Phys.* **96**, 4215 (1992)

[6] G Coulston and K Bergmann, *J. Chem. Phys.* **96**, 3467 (1992)

[7] J Oreg, K Bergmann, B W Shore and S Rosenwaks, *Phys. Rev.* **A45**, 4888 (1992)

[8] B W Shore, K Bergmann, J Oreg and S Rosenwaks, *Phys. Rev.* **A44**, 7442 (1991)

[9] B W Shore, K Bergmann, A Kuhn, S Schiemann, J Oreg, and J H Eberly, *Phys. Rev.* **A45**, 5297 (1992)

[10] (a) U Gaubatz, P Rudecki, M Becker, S Schiemann, M Külz and K Bergmann, *Chem. Phys. Lett.* **149**, 463 (1988)
J R Kuklinski, U Gaubatz, F T Hioe and K Bergmann, *Phys. Rev.* **A40**, 6741 (1989)
G-Z He, A Kuhn, S Schiemann and K Bergmann, *J. Opt. Soc. Am.* **B71**, 1960 (1990)
(b) U Gaubatz, P Rudecki, S Schiemann and K Bergmann, *J. Chem. Phys.* **92**, 5363 (1990)
(c) H-G Rubahn, E Konz, S Schiemann and K Bergmann, *Z. Phys.* **D22**, 401 (1991)

[11] B W Shore, J Martin, M P Fewell and K Bergmann, *Phys. Rev.* **A52**, 566 (1995)

[12] J Martin, B W Shore and K Bergmann, *Phys. Rev.* **A52**, 583 (1995)

[13] J Martin, B W Shore and K Bergmann, *Phys. Rev.* **A54**, 1556 (1996)

[14] S Ghosh, S Sen, S S Bhattacharyya and S Saha, *Phys. Rev.* **A59**, 4457 (1999)

[15] H Abgrall, F Launay, E Roueff and J-Y Roncin, *J. Chem. Phys.* **87**, 2036 (1987)

[16] L Wolniewicz and K Dressler, *J. Chem. Phys.* **88**, 3861 (1988); **85**, 2821 (1986)

[17] W Kolos, K Szalewicz and H Z Monkhorst, *J. Chem. Phys.* **84**, 3278 (1986)
W Kolos and L Wolniewicz, *J. Chem. Phys.* **41**, 3663 (1964)
A L Ford, A M Greenawalt and J C Browne, *J. Chem. Phys.* **67**, 983 (1977)

[18] L Wolniewicz, *J. Chem. Phys.* **51**, 5002 (1969)

[19] N E Greville, in *Mathematical methods for digital computers* edited by A Ralston and H S Wilf (Wiley, New York, 1967) vol. 2, p. 156

[20] J W Cooley, *Math. Comput.* **15**, 363 (1961)

[21] A C Allison and A Dalgarno, *At. Data* **1**, 289 (1970)
T L Stephens and A Dalgarno, *J. Quant. Spectrosc. Radiat. Trans.* **12**, 569 (1972)

[22] H Daido, E Miura, Y Kitagawa, Y Kato, K Nishihara, S Nakai and C Yamanaka, in *Short-wavelength lasers and their application*; edited by C Yamanaka (Springer, Berlin, 1988), p. 105

[23] S C Wallace, *Photophysics and photochemistry in the vacuum ultraviolet* edited by S P Mc Glynn, G L Findley and R H Hubener (Reidel, Holland, 1985) p. 105